Al/Ti contacts to Sb-doped *p*-type ZnO

L. J. Mandalapu, F. X. Xiu, Z. Yang, and J. L. Liu[a)]
Quantum Structures Laboratory, Department of Electrical Engineering, University of California at Riverside, Riverside, California 92521

(Received 23 April 2007; accepted 19 June 2007; published online 30 July 2007)

Sb-doped *p*-type ZnO film was grown on Si (100) substrate by molecular-beam epitaxy. Al/Ti metal was evaporated on the ZnO film to form contacts. As-deposited contacts were Schottky with a barrier height of 0.8 eV. Ohmic conduction was achieved after thermal annealing. The different combinations of Ohmic and Schottky contacts on Sb-doped ZnO layer led to metal-semiconductor-metal (MSM), Schottky, and photoconductive devices. Ohmic contacts on Sb-doped *p*-type ZnO and backside of *n*-type Si substrate formed a heterojunction diode. MSM, Schottky, and photoconductor devices exhibited typical electrical characteristics, however, inverted rectification was observed for heterojunction diodes. All devices exhibited ultraviolet (UV) photoresponse. Secondary ion mass spectroscopy measurements were performed on the Ohmic and Schottky contacts on Sb-doped ZnO film to trace the metal profiles before and after annealing. Mechanisms of the formation of Schottky and Ohmic contacts to Sb-doped *p*-type ZnO and their device operation principles are discussed. This work suggests that Al/Ti can be used as both Ohmic and Schottky contacts to Sb-doped *p*-type ZnO for UV detection applications. © *2007 American Institute of Physics*. [DOI: 10.1063/1.2759874]

I. INTRODUCTION

ZnO shows great promise for the application of ultraviolet (UV) optoelectronic devices due to its intrinsic properties such as wide band gap and large exciton binding energy.[1–3] However, lack of reliable *p*-type doping of ZnO has hindered the progress of ZnO-based optoelectronics. Much effort is needed to enhance the performance of the existing devices.[4–10] Our group recently reported reliable and reproducible *p*-type ZnO films on Si (100) substrates using Sb doping.[11] We also fabricated $p-n$ heterojunction photodiode based on *n*-Si (100) (Ref. 12) and homojunction photodiode on Si (111) (Ref. 13) employing the Sb-doped *p*-type films, which showed good device characteristics. Studies on contacts to other ZnO-based materials have been performed in order to achieve devices with optimized performance.[14–19] To explore Sb-doped ZnO films further for various device applications in this article, we follow up with our previous studies[12] and report systematically fabrication and characterization of both Ohmic and Schottky contacts to Sb-doped *p*-type ZnO films grown on *n*-Si substrate using Al/Ti metal. Current-voltage ($I-V$) and photocurrent (PC) characterization of four types of resulting devices namely, metal-semiconductor-metal (MSM) detector, Schottky photodiode, photoconductor, and heterojunction diode were carried out.

II. EXPERIMENTAL SECTION

Sb-doped ZnO thin film was grown on *n*-Si (100) substrate with resistivity of 20–30 Ω cm using an electron-cyclotron-resonance (ECR)-assisted molecular-beam epitaxy (MBE) system. Detailed growth procedures can be found elsewhere.[11,12] In brief, Zn and Sb were provided by low-temperature effusion cells. Oxygen plasma was generated using an ECR tube. Substrate temperature and Sb cell temperature were kept at 550 °C and 350 °C, respectively during the growth of Sb-doped ZnO layer. The sample was finally annealed *in situ* at 650 °C for 30 min under vacuum to activate the Sb dopants. The thickness of the resultant ZnO layer is around 200 nm. Hall effect measurement shows that the Sb-doped ZnO layer exhibits a hole concentration, mobility, and resistivity of 1.0×10^{18} cm^{-3}, 22.4 $cm^2\ V^{-1}\ S^{-1}$, and 0.27 Ω cm, respectively at room temperature. To study metal contacts and properties of their combinations, Al/Ti metal contact pairs with thickness of 400/10 nm and dimension of 600×600 μm^2 were evaporated on the Sb-doped ZnO layer. As-deposited contacts were Schottky that resulted in MSM device. Photoconductor devices were fabricated by making both the contacts Ohmic through thermal annealing at 650 °C for 30 s in N_2 environment. To fabricate the Schottky diode, one contact of each pair was evaporated first and annealed to become Ohmic, followed by deposition of another contact of the pair, which was Schottky due to *as*-deposited conditions. Secondary ion mass spectroscopy (SIMS) was used to obtain the elemental profiles from the *as*-deposited and annealed contact samples. Additionally, heterojunction diodes were formed with Ohmic contacts to the backside of *n*-Si substrates and on ZnO layer. $I-V$ measurements were carried out using an Agilent parameter analyzer 4155C and a Signatone probe station. Capacitance-voltage ($C-V$) characterization was made using Agilent 4284A precision LCR meter at 1 MHz. Spectral response of the photodetector devices was obtained using a home-built

[a)]Electronic mail: jianlin@ee.ucr.edu

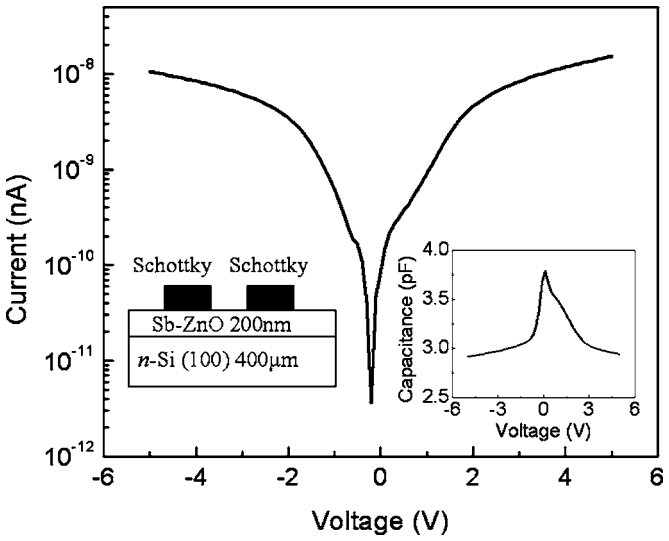

FIG. 1. $I-V$ characteristics of the MSM device on semilogarithmic scale. Inset on left is the cross sectional schematic of the device and the right inset shows $C-V$ characteristics.

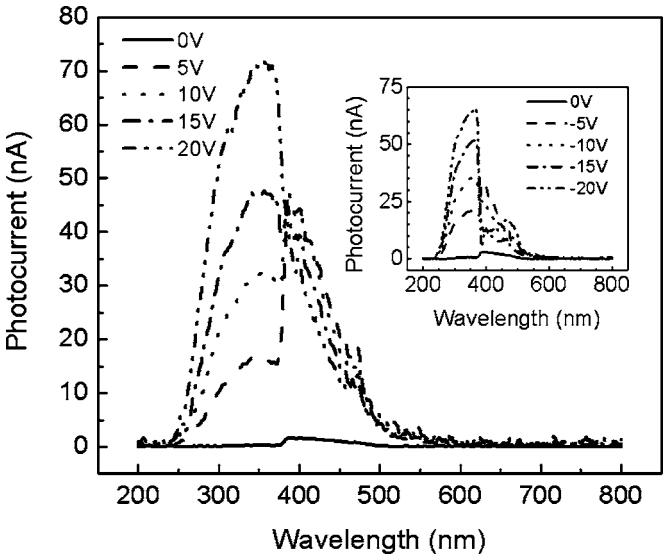

FIG. 2. Voltage dependent PC spectra of the MSM detector in positive bias region and inset shows the PC spectra for negative bias.

PC measurement system including a Xe arc lamp, a monochromator, and a lock-in amplifier.

III. RESULTS AND DISCUSSION

Figure 1 shows the $I-V$ characteristics of two *as*-deposited contacts (a MSM device) measured in dark on a semilogarithmic scale, in which the absolute value of current is shown. The schematic of the device is shown as the left inset of Fig. 1. The $I-V$ curve clearly exhibits nearly symmetric characteristics with a barrier for either polarity of biasing. Dark current is low of the order of nA with a value of about 1.0×10^{-8} A for −5 V bias. The $C-V$ curve obtained in dark is shown as the right inset of the Fig. 1. At zero bias, the capacitance is determined by the built-in depletion width. As the bias is increased, the depletion region of the reversely biased metal/semiconductor contact widens, resulting in the decrease of capacitance. Capacitance is eventually saturated when the active region is completely depleted. Similar to the symmetric nature of $I-V$ characteristics, the $C-V$ curve is also similar for both the positive and negative biasing regions.

Figure 2 and its inset show voltage dependent PC spectra of the MSM device in both the positive and negative biasing regions, respectively. Almost identical photoresponse is observed under the positive and negative biasing conditions. UV response is clearly observed with the absorption edge at 366 nm (3.38 eV). This wavelength is corresponding to the band gap of ZnO. The UV response below 366 nm is primarily due to the excitation of electrons from the valence band to the conduction band. Response beyond this wavelength also occurs, which is mainly attributed to the photoexcitation of carriers in the Al/Ti metal to ZnO by thermionic emission over the Schottky barrier. In addition, the photoexcitation of carriers from deep levels in ZnO and from Si substrate may also contribute to the response in this region.[13] The PC in the UV region depends on the bias voltage more dramatically than the PC in the visible region. This suggests that the film quality of ZnO is good and the band-to-band absorption dominates among all possibilities.

In Fig. 3, rectifying dark $I-V$ characteristics of the fabricated Schottky diode is shown on a semilogarithmic scale. The left inset shows the cross-sectional schematic of the Schottky diode with one Schottky and another Ohmic contact on ZnO. Because the device is a *p*-type Schottky diode, negative bias was applied to the unannealed Schottky contact of the device during $I-V$ measurements. The forward $I-V$ characteristics follow the relation for the thermionic emission over a barrier

$$J_F = A^*T^2 \exp(-e\Phi_b/kT)[\exp(eV/nkT) - 1], \quad (1)$$

where, J_F is the current density, A^* is the Richardson's constant for *p*-ZnO, T the absolute temperature, e the electronic

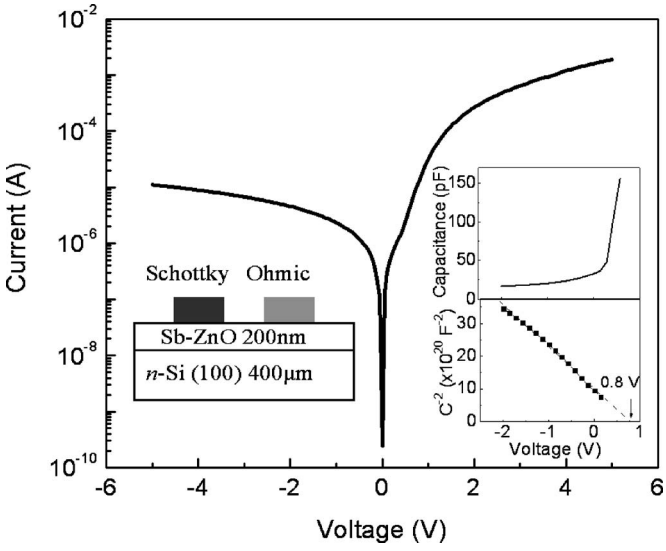

FIG. 3. $I-V$ characteristics of the Schottky diode on semilogarithmic scale with left inset showing cross-sectional schematic of device with one Schottky and another Ohmic contact. Right inset shows the $C-V$ and $1/C^2-V$ curves of the same diode.

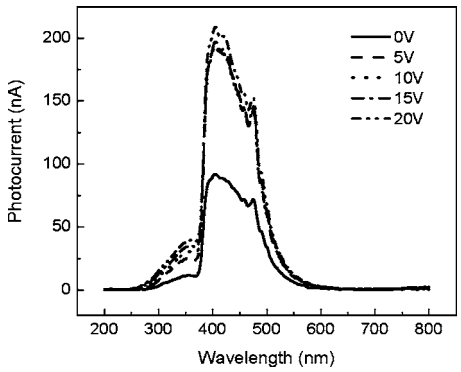

FIG. 4. Voltage dependent PC spectra of the Schottky photodiode.

charge, Φ_b the barrier height, k the Boltzmann's constant, n the ideality factor, and V the applied voltage. Since the actual area of the device is not known, the $I-V$ characteristics could not be fitted to obtain the ideality factor or precise barrier height. Turn-on voltage is estimated to be around 1 V and the dark current is about 1.1×10^{-5} A for 5 V reverse bias. $C-V$ characteristic of the Schottky device is shown in the upper-right inset of Fig. 3. The diffusion capacitance in the forward bias is high and the depletion capacitance in the reverse bias decreases with increase in the reverse voltage. $1/C^2$ plot against reverse bias voltage shows a linear trend, extrapolating which a barrier height of about 0.8 eV is estimated as shown in the lower-right inset of the figure. This barrier height is close to the turn-on voltage estimated from the $I-V$ characteristics.

Voltage dependent PC spectra of the Schottky diode are shown in Fig. 4. Good response in both UV and visible regions was observed. Again, the absorption below 366 nm is mainly due to band-to-band absorption in ZnO while the absorption above 366 nm is due to the thermionic emission of carriers in Al/Ti metal to ZnO, absorption in deep levels in ZnO and the Si substrate. The photoresponse below 366 nm increases with the increase of bias voltage while the response in the visible region begins to saturate for large reverse bias.

Figure 5 shows dark $I-V$ characteristics of the photoconductive device consisting of two Ohmic contacts. The left inset in Fig. 5 gives the cross sectional schematic of the photoconductor device. Linear characteristics, especially at low bias voltages confirm the establishment of Ohmic contacts. The figure is plotted on a log-log scale by using absolute values of current and voltage, which shows equal magnitude of both the forward (dotted) and reverse (solid lines) currents at a given bias voltage. Dark current is about 2 mA for a 5 V bias. The contact resistance is estimated to be around 915 Ω from the plot of contact resistance against inter-contact distance shown in the right inset of Fig. 5. Relatively low contact resistance is due to high-temperature annealing at 650 °C. Higher-temperature annealing was avoided to prevent the degradation of contacts. The specific contact resistivity is about 22 Ω cm^2 while the sheet resistance is 170 Ω/sq using TLM measurements.

Figure 6 shows voltage dependent PC spectra of the photoconductor. Large dark current limited the collection of photocarriers at high bias voltages. The photoresponse of the photoconductor also follows a similar trend of the MSM device, where, the ratio of the PC below and above 366 nm is high for increasing bias voltages. This is again due to efficient collection of photogenerated carriers in conduction and valence band rather than deep levels.

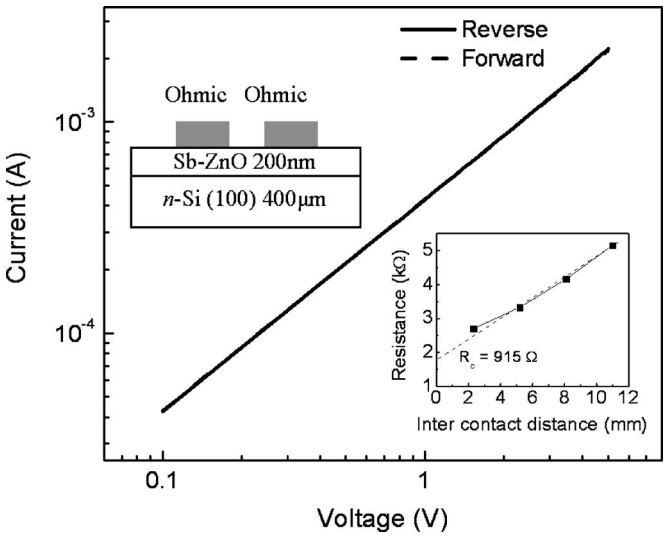

FIG. 5. Linear $I-V$ characteristics of the photoconductor on log-log scale. Left inset shows cross sectional schematic of the device while right inset shows the intercontact resistance as a function of contact spacing.

The fourth contact pair involving Ohmic contacts to the backside of Si substrate and on p-type ZnO lead to p-ZnO/n-Si heterojunction device (top-left inset in Fig. 7). $I-V$ characteristics of this device exhibited interesting inverted rectification as shown in Fig. 7. Due to the band alignment, a quantum well for holes is formed in equilibrium on the n-Si side as seen in the right inset of Fig. 7. Hence, the narrow band gap Si is inverted in the interface when connecting to p-ZnO. During the forward operation of the heterojunction diode (positive bias on n-type Si), holes will overcome a "Schottky barrier" (effective band offset in the valence band edge, or the Fermi level in the inverted Si quantum well to the valence band edge of ZnO in the interface). In other words, holes are from Si to ZnO, rather than in the opposite direction in this forward operation. The positive voltage polarity on n-type Si results in the rectifying characteristics. The turn-on voltage or the barrier height of the device was estimated from $I-V$ and $C-V$ (not shown here) characterizations to be about 1.6 eV, which is slightly

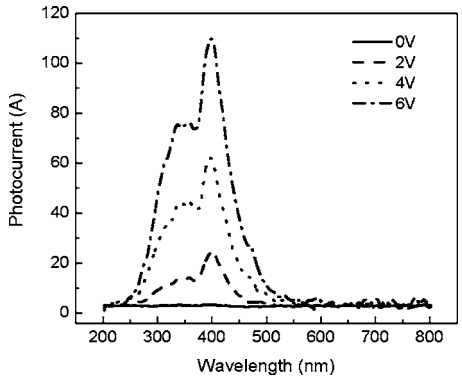

FIG. 6. Voltage dependent PC spectra of the photoconductive device.

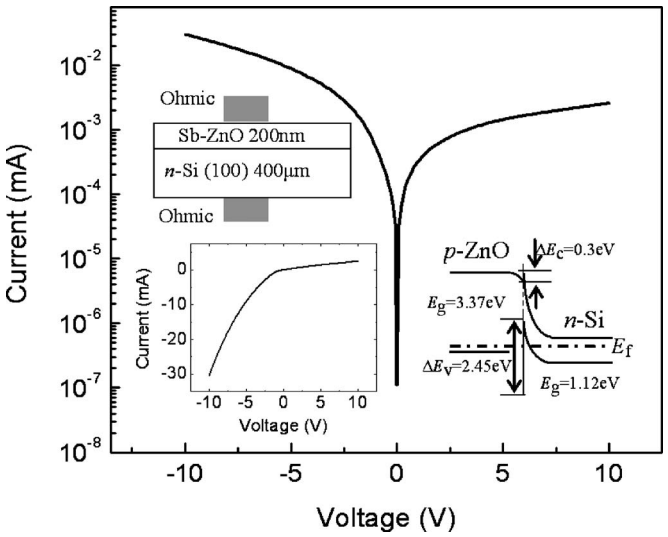

FIG. 7. $I-V$ characteristics of heterojunction diode on a semilogarithmic scale. Insets show cross sectional schematic and band diagram of the device.

smaller from the value reported earlier.[12] The possible reason may be due to smaller contact resistance of 915 Ω in the current study compared to 5.1 kΩ recorded previously since those Ohmic contacts were formed at different annealing conditions. There is not much electron transport in this bias condition making it a "*p*-type diode" with unipolar hole transport rather than bipolar transport in a regular diode, therefore, it "behaves" like a *p*-type Schottky diode. During the reverse operation of our diode (positive on *p*-type ZnO), the current appears to be saturated in a linear plot (bottom-left inset), such as the reverse bias characteristics of a normal diode. Nevertheless, it is evident in the semilogarithmic plot that the amplitude of the current increases as the reverse bias increases. This is a typical characteristic of nonidealized leakage current such as recombination current. The reason of forming this recombination leakage current in our diode is that this voltage polarity has to first convert the inverted Si (the interface) to depletion, and then to normal when the injected electrons from *n*-Si recombine with holes in the quantum well before the holes from *p*-type ZnO have available states to move on. In addition, high-density dislocations in this heteroepitaxial film also lead to leakage current. Therefore, this bias condition results in limited current mainly due to recombination current.

Voltage dependent PC spectra are obtained by applying positive on the *p*-type Sb-doped ZnO layer of the diode as shown in Fig. 8. Good detection is observed in both UV and visible region. However, unlike other three devices, response in both the regions increases identically with increasing bias. This indicates that the interface of ZnO and Si and Si substrate play a major role in the visible light detection of heterojunction diode. For MSM, Schottky and photoconductor devices Si substrate is not an active layer.

Finally, to understand the formation of Schottky and Ohmic contacts of Al/Ti metal on the Sb-doped *p*-type ZnO films, SIMS was used to obtain various elemental profiles of the contacts before and after annealing as shown in Figs. 9(a) and 9(b), respectively. The *as*-deposited sample has well defined Al and Ti layers on ZnO, indicating negligible metal

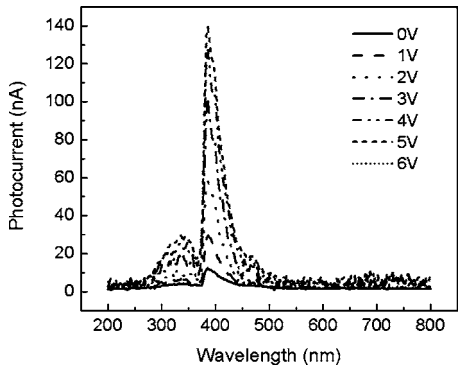

FIG. 8. PC characteristics of heterojunction diode obtained by applying various reverse (positive bias on *p*-type Sb-doped ZnO layer) voltages.

diffusion into ZnO film. In general, Al/Ti has a work function that aligns near the conduction band edge of ZnO. This suggests that ideal Al/Ti to *p*-ZnO contact should have Schottky barrier height of about 3.4 eV or so.[20] Nevertheless, in both $I-V$ and $C-V$ measurements, Schottky barrier height of about 0.8 eV was obtained. This phenomenon is due to high-density surface states of the Sb-doped *p*-type ZnO that pin the Fermi level in the metal-semiconductor interface. In other *p*-type wide-band gap semiconductors, such effect was often observed. After annealing, as shown in Fig. 7(b), no evident Al diffusion was observed as Ti layer acts as a barrier to prevent Al from diffusing into ZnO film, thus, avoiding the conduction-type conversion. The SIMS profile of the annealed sample also shows out diffusion of Zn, which induces more Zn vacancies locally.[18] The Zn vacancies by themselves form relatively deep acceptor levels. However, some of these may connect with Sb_{Zn} to form $Sb_{Zn}+2V_{Zn}$ complexes, which are shallow acceptors.[11,21] The local increase in hole concentration reduces the Schottky barrier width further and Ohmic tunnel junction contacts are formed.

IV. CONCLUSION

In summary, Al/Ti Ohmic and Schottky contacts to Sb-doped *p*-type ZnO were fabricated. The combinations of

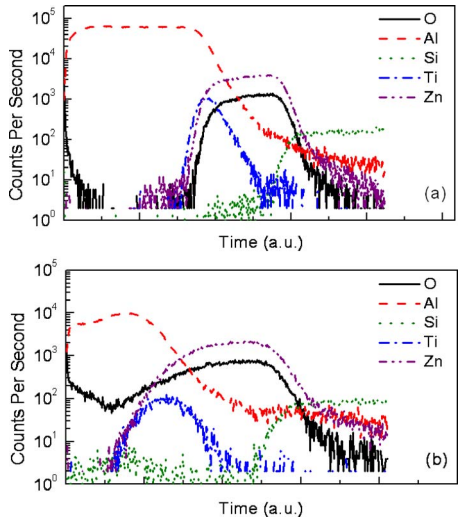

FIG. 9. (Color online) (a) Elemental profile of Al/Ti contacts on Sb-doped ZnO sample (a) *as*-deposited, and (b) after annealing at 650 °C for 30 s, using secondary ion mass spectroscopy.

these contacts result in MSM device, Schottky diode and photoconductor that show typical $I-V$, $C-V$, and photoresponse characteristics. Heterojunction p-ZnO/n-Si diode exhibits inverse rectifying behavior, which may be understood from the picture of inverted Si in the ZnO/Si interface. Schottky barrier height of about 0.8 eV was observed as a result of surface states. Ohmic contacts were formed under thermal annealing. The out diffusion of Zn leads to more local Zn vacancies, which connect with Sb_{Zn} to form additional shallow acceptor states ($Sb_{Zn}+2V_{Zn}$), thereby forming thinner Schottky barrier and Ohmic tunnel contact.

ACKNOWLEDGMENTS

This work was supported by the DoD/DMEA through the center for NanoScience and Innovation for Defense (CNID) under the award number H94003-06-2-0608. We would like to acknowledge the SIMS measurements performed by Mikhail Klimov, Materials Characterization Facility, AMPAC, University of Central Florida.

[1]D. C. Look, Mater. Sci. Eng., B **80**, 383 (2001).
[2]S. J. Pearton, D. P. Norton, K. Ip, and Y. W. Heo, J. Vac. Sci. Technol. B **22**, 932 (2004).
[3]U. Ozgur, Ya. I. Alivov, C. Liu, A. Teke, M. A. Reshchikov, S. Dogan, V. Avrutin, S. J. Cho, and H. Morkoc, J. Appl. Phys. **98**, 041301 (2005).
[4]Y. I. Alivov, J. E. V. Nostrand, D. C. Look, M. V. Chukichev, and B. M. Ataev, Appl. Phys. Lett. **83**, 2943 (2003).
[5]D. Wang, Y. C. Liu, R. Mu, J. Y. Zhang, Y. M. Lu, D. Z. Shen, and X. W. Fan, J. Phys. Condens. Matter **16**, 4635 (2004).
[6]D. K. Hwang, S. H. Kang, J. H. Lim, E. J. Yang, J. Y. Oh, J. H. Yang, and S. J. Park, Appl. Phys. Lett. **86**, 222101 (2005).
[7]A. Tsukazaki, A. Ohtomo, T. Onuma, M. Ohtani, T. Makino, M. Sumiya, K. Ohtani, S. F. Chichibu, S. Fuke, Y. Segawa, H. Ohno, H. Koinuma, and M. Kawasaki, Nat. Mater. **4**, 42 (2005).
[8]T. Aoki, Y. Hatanaka, and D. C. Look, Appl. Phys. Lett. **76**, 3257 (2000).
[9]Y. R. Ryu, W. J. Kim, and H. W. White, J. Cryst. Growth **219**, 419 (2000).
[10]D. C. Look and B. Claflin, Phys. Status Solidi B **241**, 624 (2004).
[11]F. X. Xiu, Z. Yang, L. J. Mandalapu, D. T. Zhao, J. L. Liu, and W. P. Beyermann, Appl. Phys. Lett. **87**, 252102 (2005).
[12]L. J. Mandalapu, F. X. Xiu, Z. Yang, D. T. Zhao, and J. L. Liu, Appl. Phys. Lett. **88**, 112108 (2006).
[13]L. J. Mandalapu, F. X. Xiu, Z. Yang, D. T. Zhao, and J. L. Liu, Appl. Phys. Lett. **88**, 092103 (2006).
[14]S. Kim, B. S. Kang, F. Ren, Y. W. Heo, K. Ip, D. P. Norton, and S. J. Pearton, Appl. Phys. Lett. **84**, 1904 (2004).
[15]M. Kurimoto, A. B. M. A. Ashrafi, M. Ebihara, K. Uesugi, H. Kumano, and I. Suemune, Phys. Status Solidi B **241**, 635 (2004).
[16]J. H. Lim, K. K. Kim, D. K. Hwang, H. S. Kim, J. Y. Oh, and S. J. Park, and J. Electrochem. Soc. **152**, G179 (2005).
[17]S. Liang, H. Sheng, Y. Liu, Z. Huo, Y. Lu, and H. Shen, J. Cryst. Growth **225**, 110 (2001).
[18]H. S. Yang, Y. Li, D. P. Norton, K. Ip, S. J. Pearton, S. Jang, and F. Ren, Appl. Phys. Lett. **86**, 192103 (2005).
[19]K. Ip, G. T. Thaler, H. Yang, S. Y. Han, Y. Li, D. P. Norton, S. J. Pearton, S. Jang, and F. Ren, J. Cryst. Growth **287**, 149 (2006).
[20]S. M. Sze, *Physics of Semiconductor Devices*, 2nd ed. (Wiley, New York, 1981).
[21]S. Limpijumnong, S. B. Zhang, S. H. Wei, and C. H. Park, Phys. Rev. Lett. **92**, 155504 (2004).